Astron. Astrophys. 316, 555–563 (1996)

ASTRONOMY
AND
ASTROPHYSICS

Interstellar propagation of cosmic rays: analysis of the Ulysses primary and secondary elemental abundances

M.A. DuVernois, J.A. Simpson, and M.R. Thayer

Enrico Fermi Institute and the Department of Physics, 933 East 56th Street, University of Chicago, Chicago, IL 60637-1460, USA

Received 19 March 1996 / Accepted 15 July 1996

Abstract. The purpose of this investigation is to study the validity of the "leaky box" propagation model and determine some of its parameters. The pathlength distributions and their energy dependencies are derived from measurements of secondary-to-primary abundance ratios.

A special charged particle telescope carried on the Ulysses spacecraft has provided a complete separation of elements from hydrogen to nickel in the energy range $\sim$ 40 to $\sim$ 400 MeV-nucleon^{-1} in a time interval sufficient to analyze more than 4000 iron nuclei. The secondary to primary ratios of elemental abundances reported here are B/C, F/Ne, P/S, Sc/Fe, Ti/Fe, V/Fe, Cr/Fe and Mn/Fe. Two cases of the leaky box model were analyzed: 1) a single exponential, energy dependent, pathlength distribution, and 2) a double exponential energy dependent pathlength distribution. During the measurement period (1990-1995) the heliospheric level of solar modulation changed over more than a factor of two and was taken into account using a spherically symmetric model of solar modulation. The primary abundances used in our analysis are those derived from the Ulysses High Energy Telescope results obtained by DuVemois & Thayer (1996). These abundances are consistent with solar system abundances after correction for the first ionization potential (FIP) bias.

Only the single exponential pathlength distribution satisfied all the measurements from boron to iron with a mean pathlength decreasing with decreasing energy below $\sim$ 1 GeV-nucleon^{-1}. The double exponential pathlength distribution predicted much higher abundances of secondary elements than permitted by the measurements. No depletion of short patlengths was required at any energy for the Sc-Mn or Fe nuclei.

It is not certain whether the results reported here can accommodate any models of continual acceleration or reacceleration in the interstellar medium. At most, these models would have to have a very low level of acceleration.

Key words: (ISM) cosmic rays

Send offprint requests to: J.A. Simpson
(simpson@odysseus.uchicago.edu)

1. Introduction

The high energy γ-ray background from the decay of π° produced from interactions of cosmic rays is observed throughout the galactic disc. Consequently, models for the interstellar propagation of cosmic ray nuclei assume that cosmic rays also are present throughout the galaxy independent of whether their acceleration occurs in discrete sources (e.g. supernovae), by distributed shocks, or turbulence in the interstellar medium. With a galactic containment time of $\sim$ 10^7 years for propagation through an average interstellar medium density of $\sim$ 0.2–0.3 atom-cm^{-3} (Simpson & García-Muñoz 1988; Lukasiak et al. 1994) part of their propagation must include low density regions in the disc or galactic halo.

Neither a leaky box model of disc confinement nor a halo diffusion model (e.g. Ginzburg et al. 1980) are uniquely distinguishable from the analysis of secondary-to-primary element ratios, or primary to primary element ratios, given our present knowledge of nuclear interaction cross-sections for stable nuclides lighter than iron. However, the substantial fraction of propagation time required in the disc in order to produce the observed abundances of secondary elements and isotopes leads to the use of leaky box models for galactic cosmic ray propagation.

In a galactic leaky box model, a critical test is the simultaneous fit of pathlength distributions (PLD) over a wide range of primary and secondary elements, assuming that all the elements come from the same galactic source distribution. For example, the light elements (e.g., boron or carbon) represent the long pathlengths and the heavy elements (e.g., iron) represent the short pathlengths. Carbon nuclei have a fragmentation mean free path (mfp) of $\sim$ 8 g-cm^{-2}, while iron has a shorter fragmentation mfp of $\sim$ 2.6 g-cm^{-2} mainly due to the total, inelastic cross-section for iron being approximately 3 times the corresponding cross-section for carbon. Thus, the production of secondary nuclei from collisions of primary nuclei with interstellar matter during propagation yields secondary to primary abundance ratios that provide a unique experimental test for the validity of propagation models, especially the general class of leaky box models at low cosmic ray particle energies.

Table 1. Measured elemental ratios

Elements	Observed Ulysses ratio	Mean energy [MeV-nucleon^{-1}]	$\sigma(Z)$ Resolution [charge units, e]
B/C	0.248± 0.007	137	0.04
F/Ne	0.113 ± 0.007	174	0.06
P/S	0.189 ± 0.013	239	0.07
(Sc-Mn)/Fe	0.470 ± 0.011	308	0.08
Sc/Fe	0.034 ± 0.005	280	0.08
Ti/Fe	0.143 ± 0.010	290	0.08
V/Fe	0.072 ± 0.010	300	0.08
Cr/Fe	0.137 ± 0.010	310	0.08
Mn/Fe	0.088 ± 0.007	320	0.08

For either a leaky box or a halo diffusion propagation model there exists the possibility that after initial acceleration the nuclei undergo additional acceleration (reacceleration) during their lifetime in the galaxy, as suggested by Silberberg et al. (1983) to explain isotopic anomalies in the cosmic rays. Recent evidence shows that strong reacceleration for nuclei with energies $\gtrsim$ 1 GeV-nucleon^{-1} appears to be excluded (e.g., Webber et al. 1992; Seo & Ptuskin 1994). However, weak reacceleration at lower energies has been shown by Seo & Ptuskin (1994) to be possible although – as they point out – their calculated ratios of secondary to primary abundances with weak reacceleration (stochastic reacceleration by turbulence) show agreement with the experimental data "that is as good as the standard leaky box model calculations."

In this report we explore further the validity of the leaky box model concept using high resolution elemental measurements. A preliminary report has appeared in DuVemois, Simpson, & Thayer (1995). We include the element ratios F/Ne and P/S in addition to the ratios B/C, Sc/Fe, Ti/Fe, V/Fe, Cr/Fe, and Mn/Fe (Table 1).

We adopted the weighted-slab (WS) technique for solving the leaky box equations that has been used for many years (e.g., Fichtel & Reames 1968). Successive generations of computer programs implementing this technique were written at Chicago in the late 1970s and 1980s. The main parameters used in these codes include the interaction cross sections, the level of ionization energy loss and the choice of PLD. García-Muñoz et al. (1987, hereafter GM) reviewed the status of propagation models and discussed how a consistent form of the PLD was derived. They found that an energy-dependent truncation in short pathlengths was necessary to account simultaneously for both the observed sub-Fe/Fe ratio (sensitive to shorter pathlengths) and the B/C (longer pathlengths) ratios. Since that time more measurements of the relevant cross sections have been made (e.g., Webber et al. 1990) and the role of the diffuse ionized medium in cosmic ray propagation has been further investigated by Thayer (1995) and is included in the analysis reported here.

2. The experiment and the measurements

A cross-section of the cosmic ray nucleon detector carried on the international NASA-ESA spacecraft Ulysses is shown in Fig. 1a. Simpson et al. (1992) have described both the scientific objectives and instrument description of tills High Energy Telescope (HET). The HET's excellent mass and charge resolution was made possible by our development of position-sensitive, silicon detectors (PSD's), shown in Fig. 1b, and arranged in the telescope to determine the trajectories of the cosmic ray nuclei. Six 5000 μm Si detectors (K's) determine mass and charge by the multiple dE/dx vs. residual energy method. A Si detector and scintillator shield identify penetrating events.

Although not required for elemental separation, the instrumental corrections include:

- Temperature Corrections ($\sim$ 138ppm/°C) for the K detectors and electronics
- PSD rotational position errors to within $\sim 0.01°$
- Cant errors to $< 1°$ relative to the telescope axis.

Consistency constraints were imposed for energy loss in the PSD's and in the K-detector mass determination.

Examples of the HET isotopic resolution for iron and nickel have been published (Connell and Simpson 1995) illustrating, for example, the complete separation of ^{58}Ni from ^{60}Ni. As a consequence of this isotopic resolution, the shape of histograms of individual elements reflect their isotopic abundances. We show in Figs. 2a–d these element histograms with complete separation between adjoining charges. For example, in Fig. 2b, the element neon includes the integral number of events in the histogram – no background events needed to be subtracted.

Elemental resolution varies from an effective $\sigma(Z)$ of 0.04e at boron to 0.08e for iron. Our selection is made slightly better than this by using simultaneously both the charge and mass determinations to identify an element. By using data from after instrument turn-on, ignoring data during the Jovian encounter and large solar flares, and continuing until early 1995, we have a set of data for which the ratios of interest have small statistical errors and accordingly high significance. We made rigorous cuts on the consistency of energy losses and required all particle trajectories to be within the telescope acceptance cone. Over 4000 iron events survive these cuts. The resulting observational ratios are in Table 1. These ratios have been corrected to a common energy per nucleon interval and common spectral form after modulation as shown in Fig. 3 (Chenette et al. 1994; DuVemois et al. 1996). Errors include statistics, small uncertainties in the energy intervals, and the uncertainties in the spectral index.

In the energy range of our investigation ($\sim$40 to 400 MeV-nucleon^{-1}), the elemental ratios depend strongly upon the level of solar modulation. Using the IMP-8 helium flux data, we determined ϕ, the solar modulation potential, in a spherically symmetric heliospheric model (e.g., Evenson et al. 1983). This is a reasonable approximation since Ulysses measurements over the poles of the Sun indicate that modulation in the inner solar system is nearly spherically symmetric (Simpson et al. 1995a; Simpson et al. 1996). Our propagation models are evaluated for levels of modulation ranging from ϕ = 300 MV to ϕ = 2000 MV. This permits a direct comparison with measurements made at very different modulation levels. For the Ulysses data, we assigned an average modulation level of 840 MV. This

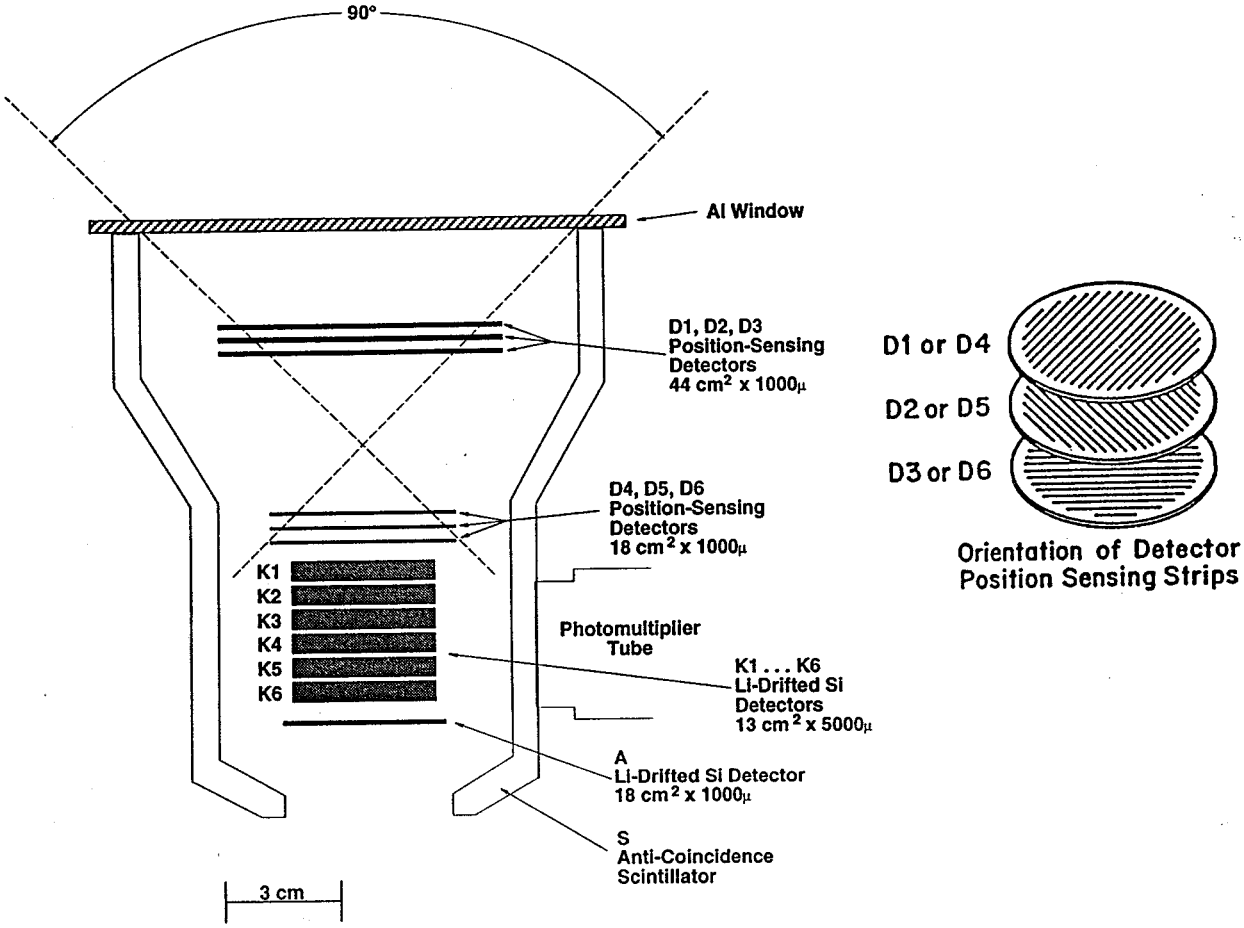

Fig. 1. a Cross section of Ulysses HET. **b** Position sensing silicon detector orientation (Simpson et al., 1992)

is determined from a weighted average, assigning to each event a modulation level appropriate to the time of the event.

To illustrate the significance of corrections for the changing level of solar modulation, we show in Fig. 4 the modulation dependence of the boron to carbon ratio at the average energy of 138 MeV-nucleon^{-1}. The curves in Fig. 4 are derived from the model calculations described in Sect. 3. The data from launch to August 1992 correspond to ϕ = 1080 MV.

The second data interval extending through February 1995 corresponds to ϕ = 600 MV, resulting in an average value of ϕ = 840 MV. In the second data interval the Ulysses spacecraft trajectory covered the range from 80° south heliospheric latitude to near equatorial (Smith et al. 1995). Over this latitude range the galactic proton spectral shape remained constant and was well described by a model spectrum resulting from a spherically symmetric modulation model (Simpson et al. 1995b).

3. Propagation model and parameters

For a detailed description of the "leaky box" equation of cosmic ray propagation see GM and references therein. If certain conditions on the cosmic ray sources, escape lifetimes, and nuclear cross sections are met, this equation is separable (Ginzburg & Syrovatskii 1964). The resulting "weighted-slab" (WS) Eq (1) can be solved as a function of pathlength traversed and energy for various assumed pathlength distributions.

$$\frac{dN_i}{dx} = \frac{\partial}{\partial E}\{(\frac{dE}{dx})_i N_i\} \qquad (1)$$
$$-\frac{N_0}{\bar{A}}\sigma_i N_i + \sum_{j\neq i}\frac{N_0}{\bar{A}}\sigma_{ij}N_j - \frac{N_i}{\gamma\beta cn\bar{A}T_i} + \sum_{j\neq i}\frac{N_j}{\gamma\beta cn\bar{A}T_j}$$

$N_i(E,x)$ is the energy and pathlength dependent abundance of the 'i'th species; σ_i, the total nuclear spallation cross-section; σ_{ij}, the partial cross-section for fragmentation of species i into species j; n the number density of the interstellar material; N_0, Avogadro's number; T_i, the half-life of radioactive species; $\bar{A}$, the mean mass of an Interstellar Medium (ISM) particle; and $(dE/dx)_i$, the mean energy loss rate due to Coulomb interactions. The number density of species i as a function of pathlength and energy $N_i(E,x)$ is then integrated over a particular pathlength PLD(E,x) distribution to deduce a local interstellar flux of species i as a function of energy, $J_i(E)$.

The assumptions which underlie the WS method have been discussed by Lezniak (1979), but there are constraints on the regimes of applicability of this technique. In particular, it can be shown that in the high-energy case where ionization energy losses are negligible, the WS technique will produce solutions

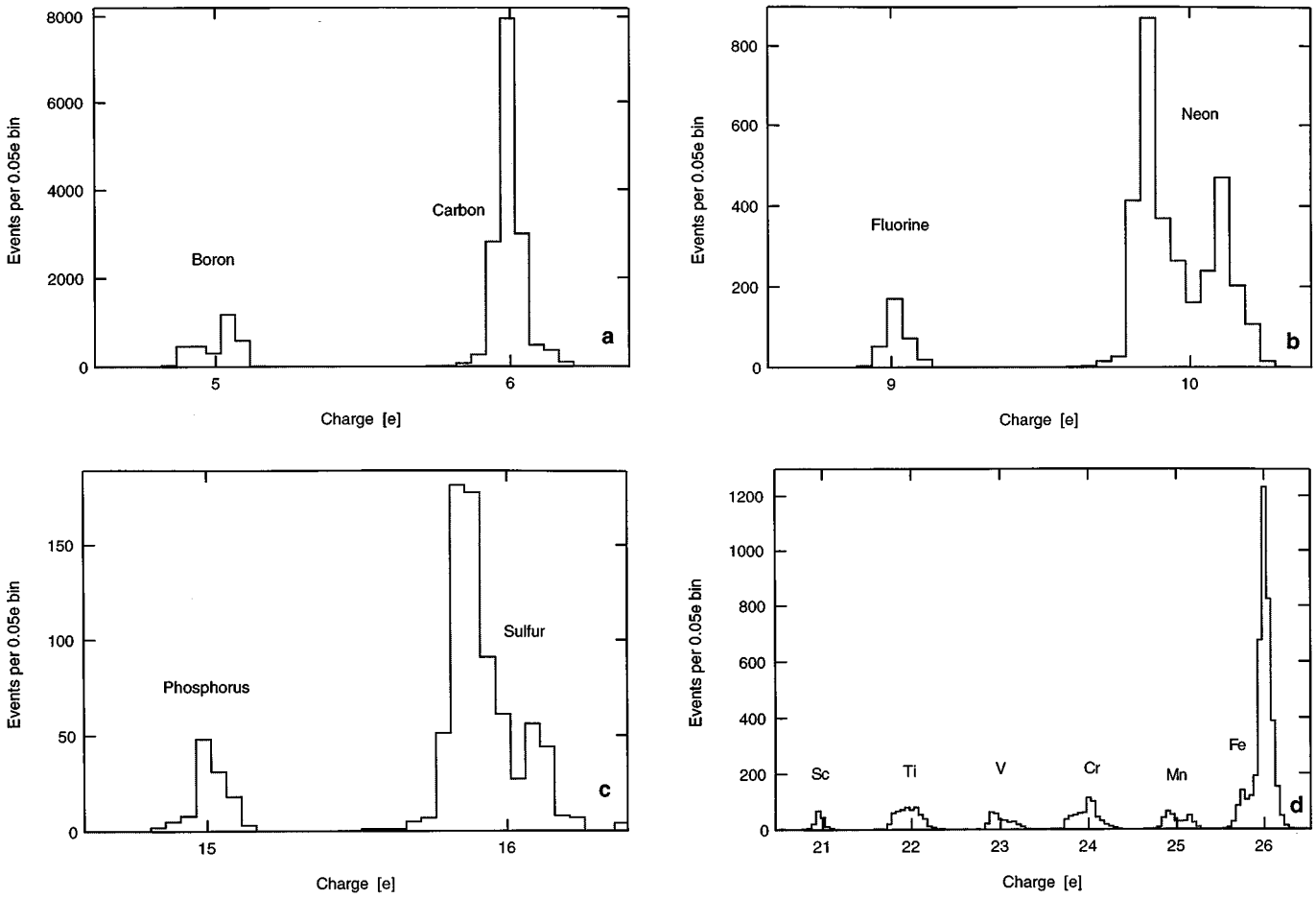

Fig. 2 a–d. Event histograms for Ulysses HET. The structure in the histograms of elements is due to the isotopic resolution in the data sets. **a** Boron and carbon, **b** fluorine and neon, **c** phosphorus and sulfur, **d** scandium through iron

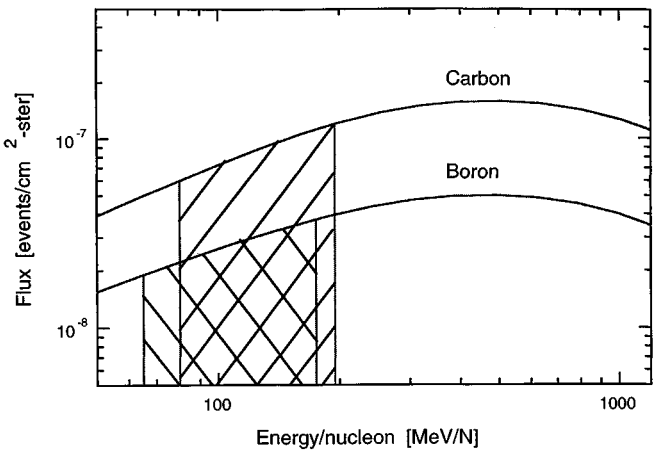

Fig. 3. Differential energy spectra for boron and carbon (Chenette et al. 1994) – cross-hatched energy intervals where Ulysses is sensitive. B/C ratio is normalized onto the overlapping energy interval

identical to that of a pure leaky box if the PLD used is a simple exponential (Lezniak 1979).

When ionization energy losses are taken into account, the WS technique is almost entirely divorced from the leaky box model unless several correction factors are included. These factors generally arise from energy-changing processes, such as ionization energy loss or the fragmentation of light particles (Beatty 1986). GM have assumed that the magnitude of these correction factors are smaller than the errors introduced in other parts of the calculation, i.e. particularly smaller than the uncertainties in the cross sections used. We make the same assumption here.

The composition of the ISM is taken to be 6.3% He by number (García-Muñoz et al. 1987), and contains an ionized HII component (Thayer 1995). The ionization loss rate due to Coulomb interactions will depend upon the ISM composition, and is found from a weighted average of the components. The importance of the HII component was recognized by Soutoul et al. (1990). We use their formulation to systematically incorporate this ionized component into our propagation calculation. Using recent values for the scale heights and densities of the ISM components (Nordgren et al. 1992; Diplas & Savage 1994; Dame et al. 1987), it is found that the energy loss rate at the energies of interest (~ 0.1–1.0 GeV nucleon^{-1}) needs to be scaled

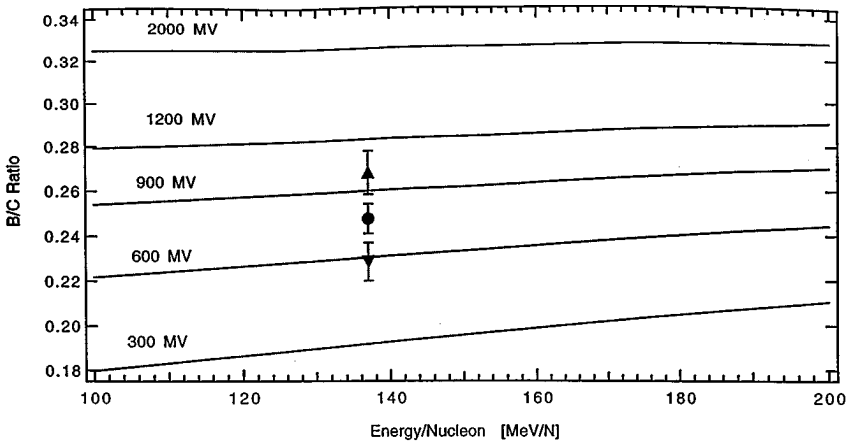

Fig. 4. Sensitivity of the Ulysses HET Boron/Carbon Ratio for selected modulation levels. Curves: SE-PLD calculation results. Data: the average value used in the present work – solid circle ($\phi = 840$ MV); upward triangle ($\phi = 1080$ MV); downward triangle ($\phi = 600$ MV)

up by a factor of approximately 1.4 over the neutral ISM composition (Thayer 1995). This corresponds to 28% of the hydrogen in the ISM being ionized on average.

The partial fragmentation cross sections used in the propagation code have also been updated since the García-Muñoz et al. work of 1987. New measurements of partial cross sections incident on hydrogen and helium targets (Webber et al. 1990) have been included in our code, along with theoretical calculations of the unmeasured cross sections (Sihver 1993). We used published total cross-sections (Karol 1975; see GM for further details). The cross sections input to our code use a weighted average (by number) of the hydrogen and helium partial fragmentation cross sections, as described in García-Muñoz et al. (1987).

4. Tests for pathlength distributions

Previous attempts to determine PLD's that meet the stringent conditions of fitting the measured secondary-to-primary abundance ratios from C to Fe began with the B/C ratio (Shapiro & Silberberg 1970). This ratio, as noted earlier, addressed the long pathlengths in the PLD. It was found to be difficult, without introducing additional parameters – such as a double exponential PLD and/or truncation of short pathlengths – to simultaneously fit the short pathlength requirement of the sub-Fe/Fe ratio (GM).

In our analysis we require the simultaneous fitting of not only the B/C and sub-Fe/Fe, but also the F/Ne and P/S ratios. Since the fluorine source abundance is consistent with zero and the phosphorus is $5.0 \pm 2.4\%$ (DuVemois & Thayer 1996) of the sulfur (compared to $\sim 1\%$ for solar system material), fluorine and phosphorus are principally secondaries in the observed cosmic ray element composition.

For our other source elemental abundance we assumed solar system abundances (Anders & Grevesse 1989) modified by the first ionization potential (FIP) bias introduced in cosmic ray abundances by the effects of charged particle acceleration (Meyer 1985; Simpson 1983; DuVemois and Thayer 1996).

We carried out our calculations for both a single and, for comparison, a double exponential PLD. The functional forms

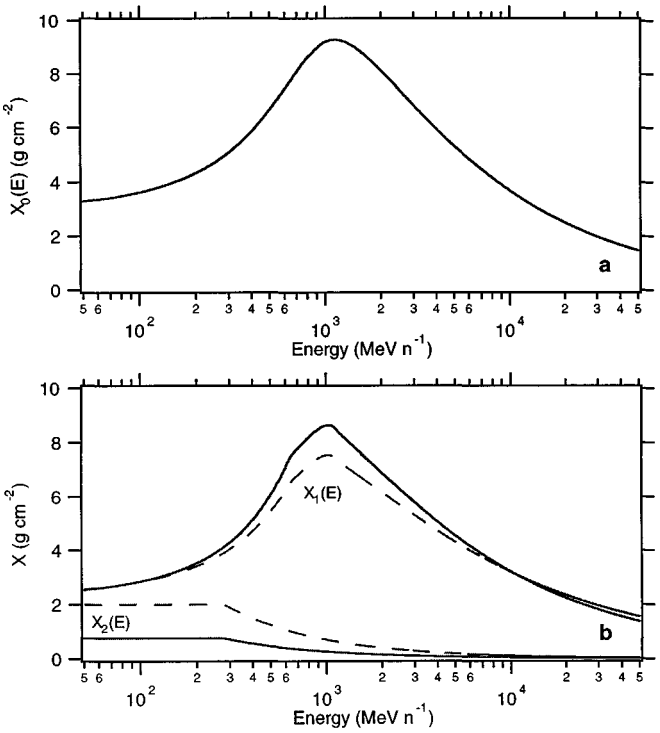

Fig. 5. a Mean X_0(E) of single exponential PLD as a function of energy. Functional form is given in the text. **b** Means X_1(E) and X_2(E) of double exponential DE-PLDS. Solid curve: means as used in text; Dashed curve: means as described by GM (1987)

are shown in Fig. 5. The mean of the single exponential PLD is given by (GM):

$$X_0(E) = A\left(\frac{T+T_0}{850+T_0}\right)^{\beta}\left[1 - 0.2\exp\left(-\left|\frac{T-850}{300}\right|\right)\right] \qquad (2)$$

where X_0 = mean of the PLD, A = normalization constant (11.0 g cm^{-2}), T is the kinetic energy per nucleon in MeV, T_0 is the nucleon rest energy (931.5 MeV), and $\beta = 0.6$ for $T > 850$ MeV nucleon^{-1} and $\beta = 2.0$ for $T < 850$ MeV nucleon^{-1}. The third factor in brackets is chosen to smooth the mean across the energy 850 MeV nucleon^{-1}. It is interesting

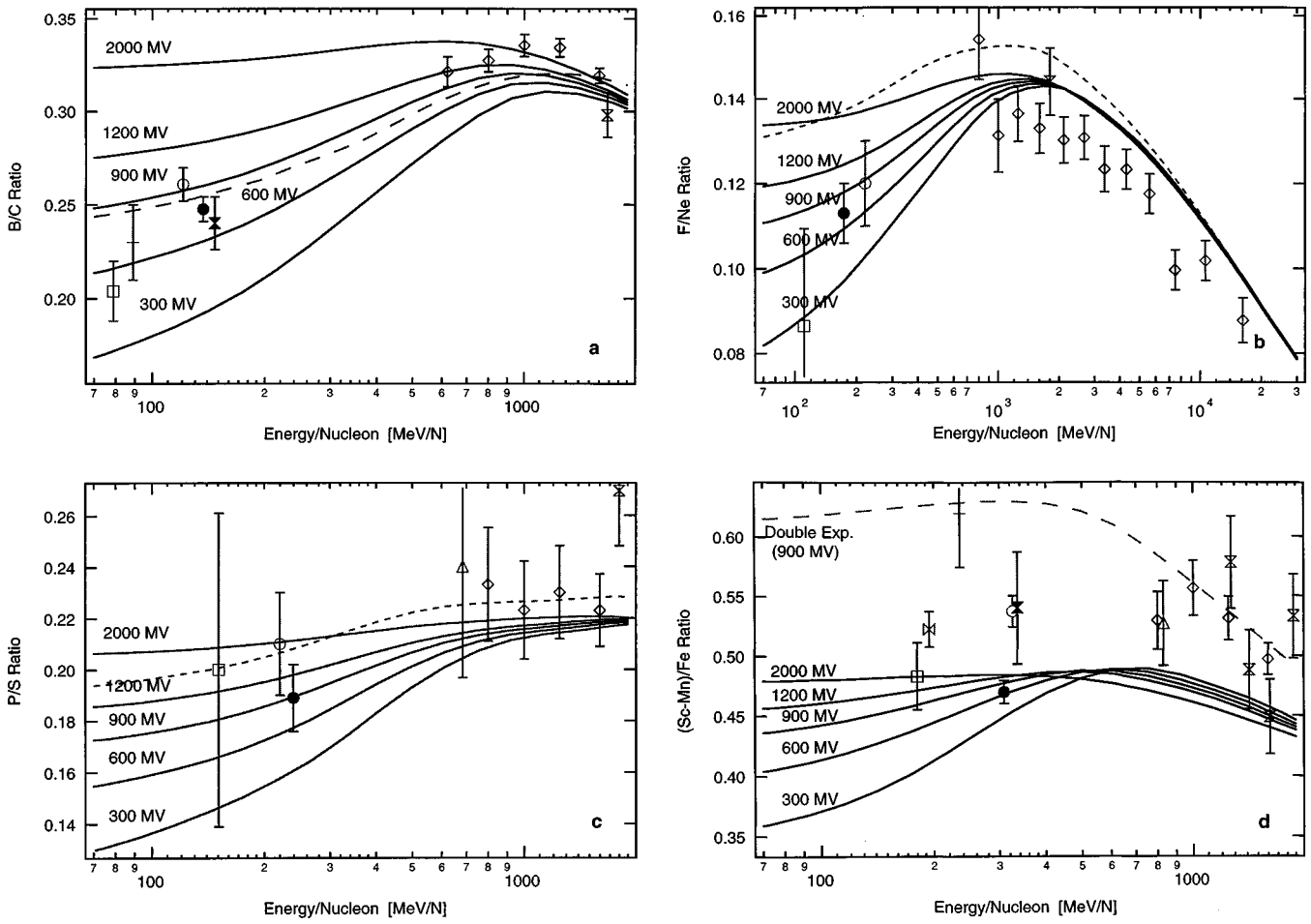

Fig. 6 a–d. Secondary/primary ratios vs. energy-nucleon for Ulysses HET and referenced experiments. Data: solid circle, this work (ϕ = 840 MV); open circle (Krombel and Wiedenbeck 1988; Leske and Wiedenbeck 1993), Leske 1993 (ϕ = 740 MV); cross, GM 1987 (ϕ = 490 MV); triangle, Esposito et al. 1992 (ϕ = 490 MV); diamond, Engelmann et al. 1990 (ϕ = 600 MV); open square, Ferrando et al.1991 (ϕ = 300 MV); open hourglass, Dwyer & Meyer 1985, 1987 (ϕ = 500 MV); filled hourglass, DuVemois et al. 1995 (ϕ = 1450 MV); supine open hourglass, Lukasiak et al. 1995 (ϕ = 500 MV). **a** Boron/carbon ratio, along with propagation calculation results (solid lines) from SE PLD. **b** Fluorine/neon ratio and SE PLD calculation results. **c** Phosphorus/sulfur ratio and SE PLD calculation results. **d** Sub-iron/iron ratio and SE PLD calculation results; DE PLD results shown as dashed line. All propagation calculations were performed at modulation levels shown on curves

to note that the peak of the PLD at around $\sim$ 1 GeV-nucleon^{-1} given in Eqn. 2, 9.2 g-cm^{-2}, is in agreement with that found by Ferrando et al. (1988) when they include a helium component in the ISM. Later reports, including those of Webber et al. (1996) have found a significantly higher PLD mean to be necessary for agreement with the B/C data, approximately 11–12.5 g-cm^{-2} at $\sim$ 1 GeV-nucleon^{-1}. This difference in escape pathlengths is undoubtedly due to differences in the parameters adopted for the calculations, such as total cross-sections and rates of ionization energy loss.

The results for a single PLD are shown in Figs. 6a–d (solid line) for the range of modulation parameter (ϕ) levels corresponding to the period 1990–1995. Note the close agreement of our experimental measurements – our average experimental value of ϕ = 840 MV – with these calculated curves. Figure 7 illustrates for B/C that the propagation results from this work match well-established measurements above $\sim$ 1 GeV-nucleon^{-1}. This is also the case for the propagations shown in Figs. 6a–d. We note that the B/C ratio curve in Fig. 4 of Webber et al. (1996) fitted to Engelmann et al. (1990) is almost identical to the ratio in Fig. 7, also fitted to the Engelmann data set. Thus, the partial cross-sections and ionization loss parameters used to derive Fig. 7 are close to those used in Webber et al. (1996).

For a mathematical description of the double exponential PLD (DE PLD) see GM. The DE PLD shown in Fig. 5 is used for comparative purposes in Figs. 6a–d. This example is more weakly truncated than the DE PLD used in GM. The solid line illustrates the means X_1 and X_2 used in this paper for the double exponential calculations, while the dashed lines illustrate the X_1 and X_2 used in GM. The "solid-line" set of PLD means has been chosen to produce agreement with the B/C and (sub-Fe)/Fe data from numerous missions, including Ulysses. In spite of the lower level of truncation there is disagreement with the F/Ne ratio (Fig. 6b) indicating no requirement for truncation.

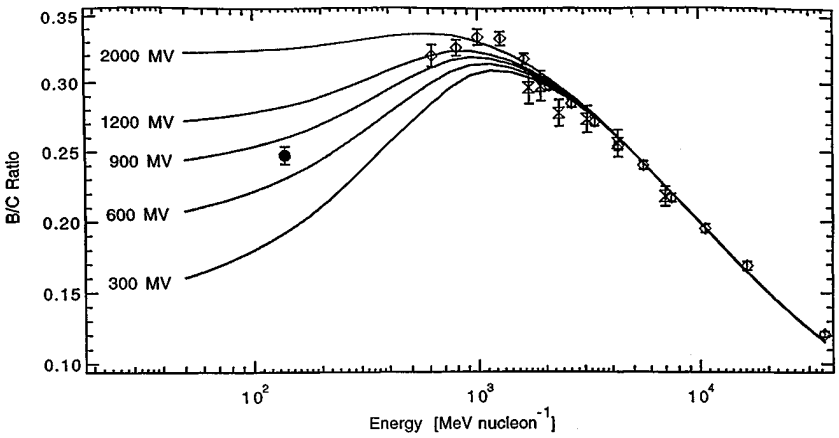

Fig. 7. Secondary/primary elemental ratio for boron and carbon. The extended energy axis shows the fit to the high energy data points. All propagation calculations were performed at the modulation levels shown on curves using the single-exponential PLD. Data: solid circle, this work (ϕ = 840 MV); diamond, Engelmann et al. 1990 (ϕ = 600 MV); open hourglass, Dwyer & Meyer 1985, 1987 (ϕ = 500 MV)

Although indistinguishable from the single experimental PLD for B/C (Fig. 6a), the double PLD model is incompatible with our measurements of the ratios of F/Ne and sub-Fe/Fe (Figs. 6b and 6d). The F/Ne and sub-Fe/Fe ratios confirm that the single PLD without significant truncation – and not a double exponential PLD – satisfies the requirements for the leaky box model.

The results in Figs. 6a–d are only weakly dependent on the form of the energy spectrum at the cosmic ray source. Following GM we adopted the form $(T + T_0)^{-\gamma}$ for the source spectrum, with T in kinetic energy per nucleon, $T_0 \sim$ 400MeV and γ = 2.6. This form of source yields a good fit after propagation and solar modulation to the measured proton and helium spectra.

As a further test to confirm that no truncation is required to account for the short pathlength of iron and sub-iron nuclei, we examined the individual sub-iron element to iron ratios for the case of the single exponential PLD shown in Fig. 8. In Fig. 6d we combined our data from Sc through Mn to Fe in order to compare the ratio with other experiments. However, as discussed by GM, the values of Mn/Fe, Cr/Fe, and Ti/Fe source ratios result in an important difference in the calculated sub-Fe/Fe ratio. They have only a small effect on the Sc/Fe and V/Fe ratios – which are nearly pure secondary ratios. These Sc/Fe and V/Fe ratios measured independently confirm that no truncation of short pathlengths is required to satisfy propagation in leaky box models of galactic propagation.

5. Discussion and conclusions

The development of a Charged Particle Telescope with excellent mass and charge resolution, for the first time, made it possible to completely separate the fluxes of all elements up to and including the iron group elements. The measurements in this report were carried out on the Ulysses spacecraft from launch in October 1990 through February 1995 – during which time the solar modulation decreased from ϕ = 1250 MV to ϕ = 600 MV, with an average value of ϕ = 840 MV – with more than 4000 Fe nuclei analyzed. This data set enabled us to test the validity of leaky box models for the galactic propagation of cosmic ray nuclei from boron to iron.

Extensive earlier research had focused on both the functional form of the pathlength distribution and the requirement for truncation, or elimination of short pathlengths, to account for measurements of the sub-Fe and Fe elements at low energies. The most comprehensive review of these questions appeared in GM with the conclusion that a depletion of short pathlengths at low energies was required irrespective of the model assumed for the PLD in order to satisfy observational constraints. They concluded that the PLD mean, X_0, is energy dependent below $\sim$ 1 GeV-nucleon^{-1} and decreases with decreasing energy. GM noted difficulty in accommodating the measured heavy nuclei secondaries and Fe measurements in the propagation models.

To test the leaky box model, we chose for analysis two cases – namely, a single exponential pathlength distribution and a double pathlength distribution with $X_0 \propto E^2$ at low energies. Only the single pathlength distribution satisfied all the measurements from boron to iron. We concluded that the mean pathlength decreased with decreasing energy below $\sim$ 1 GeV-nucleon^{-1}. Furthermore, no energy dependent depletion of short pathlength was required at any energy for either the Fe or sub-Fe nuclei. We were able, for the first time, to determine significant values for the ratios F/Ne and P/S, which placed additional constraints on propagation models and confirmed that no depletion of short patwengths was required. This conclusion is in agreement with Webber (1993).

It is important to note that whereas the IMP-8 measurements by García-Muñoz and Simpson (1979) and GM for sub $-$ Fe/Fe = 0.62 ± 0.04 at 236 MeV-nucleon^{-1}, the Ulysses measurements reported herein were sub $-$ Fe/Fe = 0.47 ± 0.01 at a comparable energy (308 MeV-nucleon^{-1}). There is an anomalously large distribution in the Sc-Mn/Fe ratios shown in Fig. 6d. These values from IMP-8, ISEE-3, Voyager, CRRES, and Ulysses are dependent on the assumed modulation levels at the time of measurement. Differences in these factors may partially account for the reported wide distribution of these values.

It is uncertain whether the experimental results we report will also accommodate models including reacceleration in the interstellar medium. For the light nuclear species that are the most sensitive indicators for reacceleration, we point out that the

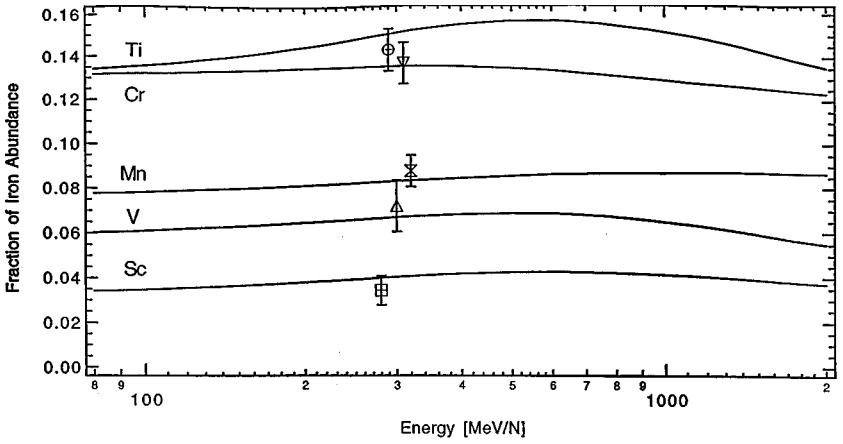

Fig. 8. The ratio of the individual subiron elements to iron. The curves represent the propagation results of the indicated species using a single exponential PLD and a modulation of ϕ = 840 MV. Data: all from Ulysses (this work); open circle, titanium; downward triangle, chromium; hourglass, manganese; upward triangle, vanadium; square, scandium

previous and present measurements satisfy both leaky box models without reacceleration and those including a small amount of reacceleration (e.g., Seo & Ptuskin 1994). On the other hand, Seo and Ptuskin and others have had difficulty fitting their models including reacceleration with the data compiled by GM for the sub-Fe to Fe ratios – a ratio derived principally from the IMP-8 measurements that we find differ from our lower Ulysses results by at least 20 percent. The Ulysses data would be consistent with the calculated curve of Seo and Ptuskin in their Fig. 9, except for their requirement of truncation of short pathlengths.

Webber et al. (1992) in their study of primary-to-primary ratios at low energy also note that including reacceleration in a leaky box model is indistinguishable from leaky box models without reacceleration. It is our view that only by investigating the radioactive isotope primaries and secondaries will the physics of propagation into the halo, and/or models including reacceleration, be distinguished within the general class of leaky box models.

Our method of analysis in reaching the conclusion that a single distribution without low energy truncation assumed galactic source elemental abudances adjusted by first ionization potential biases. These results on secondary/primary ratios complement the results on primary/primary ratios (DuVemois and Thayer 1996) which have shown that the source elemental abundances are consistent with solar system abundances after the correction for FIP is taken into account. This in agreement with the results of other investigations (Leske 1993; Webber 1993).

Acknowledgements. This research is supported in part by Ulysses NASA/JPL Contract 955432, NASA Grant NAG 5-706 and CRRES ONR Contract N00014-94-1-0868. We acknowledge the assistance of J.J. Connell in preparing the Ulysses flight data used in this work and he, M. García-Muñoz, and J. Wefel for their comments. The comments of P. Ferrando were appreciated. Special acknowledgments also go to C. Lopate and E. Murphy for their assistance with the CRRES and IMP-8 data preparation. MRT acknowledges support from NASA GSRP NGT-51300. All data from the figures and table in this paper can be found on the world wide web at http://astro.uchicago.edu/home/web/duvernoi/secprim.html along with the necessary documentation.

References

Anders E., Grevesse N., 1989, Geochim.Cosmochim.Acta. 53, 197
Beatty J.J., 1986, ApJ 311, 425
Connell J.J., Simpson J.A., 1995, 24th Intemat. Cosmic Ray Conf (Rome) 2, 602
Chenette D.L. et al., 1994, IEEE Trans. Nucl. Sci. 41, 2332
Dame T.M. et al., 1987, ApJ 322, 706
Diplas A., Savage B. ., 1994, ApJ 427, 274
DuVernois M.A., García-Muñoz M., Pyle K.R., Simpson J.A., Thayer M. R., 1996, ApJ, 466, 457
DuVernois M.A., Simpson, J.A., Thayer M.R., 1995, 24th ICRC (Rome) 2, 589
DuVernois M.A., Thayer M.R., 1996, ApJ, 465, 982
Dwyer R., Meyer P., 1985, ApJ 294, 441
Dwyer R.,Meyer P., 1987, ApJ 322, 981
Engelmann J.J. et al., 1990, A&A 233, 96
Esposito J.A. et al., 1992, Astropart. Phys. 1, 33
Evenson P. et al., 1983, ApJ 275, L15
Ferrando P. et al., 1988, Phys. Rev. C 37, 1490
Ferrando P. et al., 1991, A&A 247, 163
Fichtel C.E.,Reames D.V., 1968, Phys. Rev. 175, 1564
García-Muñoz M., Simpson J.A., 1979, 16th ICRC (Kyoto) 1, 270
García-Muñoz M., Simpson J.A., Guzik T.G., Wefel J.P., Margolis S.H., 1987, ApJS 64,269 (GM)
Ginzburg V.I., Syrovatskii S.I., 1964, The Origin of Cosmic Rays. MacMillan, New York
Ginzburg V.I., Khazan Ya.M., Ptuskin V.S., 1980, APSS 68, 295
Karol P.J., 1975, Phys. Rev. C 11, 1203
Krombel K.E., Wiedenbeck, M.E., 1988, Ap.J. 328, 940
Leske R.A., 1993, ApJ 405, 567
Leske R.A. and Wiedenbeck, M.E. 1993, Proc. 23rd ICRC (Calgary) 1, 571
Lezniak J.A., 1979, AP&SS 63, 279
Lukasiak A. et al., 1994, ApJ 423, 426
Lukasiak A. et al., 1995, 24th ICRC (Rome) 2, 576
Meyer J.P., 1985, APJS 57, 173
Nordgren T. E., Cordes J.M., Terzian Y., 1992, AJ 104, no. 4, 1465
Seo E.S. & Ptuskin V.S., 1994, ApJ 431, 705.
Shapiro M.M., Silberberg R., 1970, Ann. Rev. Nucl. Sci. 20, 323
Sihver L. et al., 1993, Phys. Rev. C 47, 1225
Silberberg R., Tsao C.H., Letaw J.R., Shapiro M.M., 1983, Phys. Rev. Lett. 51, 1217
Silberberg R., Tsao C.H., 1990, Phys. Rep. 191, 351

Simpson J.A. 1983, Ann. Rev. Nucl. Part. Sci. 33, 323
Simpson J.A. et al., 1992, A&AS 92, 365
Simpson J.A. et al., 1995a, Sci. 268, 1019
Simpson J.A. et al., 1995b, Geophys. Res. Lett. 22, 3337
Simpson J.A. & García-Muñoz M., 1988, Sp. Sci. Rev. 46, 205
Simpson J.A., Zhang M., Bame S., 1996, APJL, 465, 69
Smith E.J., Marsden R.G., Page D.E. 1995, Sci. 268, 1005
Soutoul A., Feffando P., Webber W.R. 1990, 2 1 st ICRC (Adelaide) 3, 337
Thayer M.R., 1995, 24th ICRC (Rome) 3, 124
Webber W.R., Kish J.C., Schrier D.A., 1990, Phys. Rev. C 41, 547
Webber W.R., Feffando P., Lukasiak A. McDonald F.B., 1992, ApJ 392, L91
Webber W.R., 1993, ApJ 402, 188
Webber W.R., Lukasiak A., McDonald F.B., Ferrando, P., 1996, ApJ 457, 435